

AD-A167 263

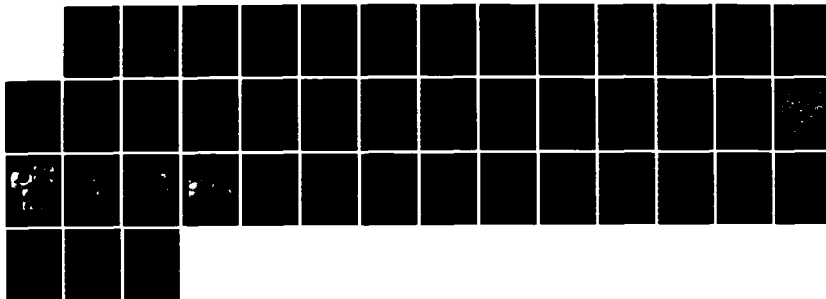
PREPARATION AND STOICHIOMETRY EFFECTS ON MICROSTRUCTURE
AND PROPERTIES OF.. (U) ILLINOIS UNIV AT URBANA DEPT OF
CERAMIC ENGINEERING R C BUCHANAN ET AL. 27 MAR 86
TR-12 N00014-80-K-0969

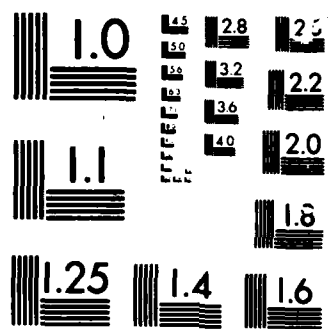
1/1

UNCLASSIFIED

F/G 7/4

NL





MICROCOPY

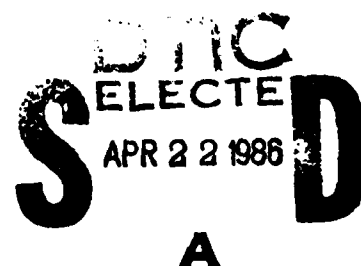
CHART

AD-A167 263

Preparation and Stoichiometry Effects on
Microstructure and Properties of High
Purity BaTiO_3

by

K. C. Buchanan and Alena K. Maurice



DNC FILE COPY

DEPARTMENT OF CERAMIC ENGINEERING
UNIVERSITY OF ILLINOIS
URBANA, ILLINOIS

This document has been approved
for public release and sale; its
distribution is unlimited.

88 4 22 1986

(12)

Final Report
Technical Report No. 12
Contract No.: US NAVY-N-00014-80-K-0969

Preparation and Stoichiometry Effects on
Microstructure and Properties of High
Purity BaTiO₃

by

R. C. Buchanan and Alena K. Maurice

March 1986

Department of Ceramic Engineering
University of Illinois at Urbana-Champaign
105 S. Goodwin Avenue
Urbana, IL 61801

Research was supported by the Office of Naval Research
Metallurgy and Ceramics Program
Department of the Navy

SELECTED
APR 22 1986
A

Production in whole or in part is permitted for any purpose
of the United States Government

This document is available for public use
distribution is unlimited

ABSTRACT

SECURITY CLASSIFICATION OF THIS PAGE

Effects of stoichiometry, precursor origin and powder synthesis method on sintered microstructure and dielectric properties of commercial high purity BaTiO_3 were examined, with a view to potential interchangeability. Powders used were prepared by conventional calcination, by precipitation from oxalate precursors and by hydrothermal synthesis.

Stoichiometric (Ba:Ti) ratios were in the range 0.987 to 1.002. Characterization by SEM, x-ray diffraction, BET surface area and particle size analysis revealed significant differences, particularly in agglomerate structure, resulting in different microstructural development. Stoichiometric effects on microstructure were also significant, if predictable. However, the combined effects of agglomerate structure and stoichiometry on measured dielectric properties could not be predicted, hence interchangeability of powders could not be achieved.



SECURITY CLASSIFICATION OF THIS PAGE

TABLE OF CONTENTS

	PAGE
I. Introduction	1
II. Experimental	4
III. Results and Discussion	5
IV. Conclusions	11
V. Acknowledgements	11
VI. References	12
VII. List of Figures	19
VIII. Summary of Work Accomplished	34
Reports	34
Theses	35
Publications	36
Technical Presentations Made (1985)	37

Preparation and Stoichiometry Effects on Microstructure and Properties of High Purity BaTiO₃

A. K. Maurice and R. C. Buchanan

1. Introduction

Commercial BaTiO₃ powders have traditionally been prepared by calcination from oxide or carbonate precursors of Ba and Ti. However, precise control of stoichiometry and powder characteristics is difficult to maintain by this technique due to a lack of consistency in raw material sources and local inhomogeneities arising from incomplete mixing and reaction of the constituents. Also, the relatively high calcination temperatures (>900°C) needed for the reaction to occur often result in the formation of coarse aggregates which can be difficult to disperse or reduce during subsequent milling. These factors can induce variations in powder characteristics which are then reflected in microstructural inhomogeneities and lack of reproducibility in the dielectric properties of the sintered ceramic.

In an effort to mitigate these effects, alternate methods of powder synthesis have been developed and described by many authors.¹⁻⁵ Typically, these have involved coprecipitation from inorganic (nitrate, chloride, sulfate) or organic (oxalate, citrate) salt solutions, from mixed alkoxide precursors or from hydrothermal solutions. Typical starting materials and reaction sequences, including calcination, are given in Table I. As indicated, the coprecipitation step is usually followed by relatively low temperature (250-750°C) decomposition and calcination reactions to form the BaTiO₃ compound. Both the oxalate and hydrothermal processes show commercial promise and are briefly described below.

Formation of BaTiO_3 by thermal decomposition of oxalate precursors, as described by Gallagher and Thompson,¹ allows for more precise control of stoichiometry and purity. Although the product is effectively formed by a solid state diffusion reaction between BaCO_3 and TiO_2 ,⁶ the resulting particles are much smaller since they are formed from crystallite sized precipitates. Lower calcination temperatures can therefore be used, which results in the formation of more reactive powders than those prepared by the conventional mixed oxide technique.⁷⁻⁹ These desirable characteristics can, however, be dissipated by the use of higher calcination temperatures than needed in order to match the processing characteristics of already established calcined powders.

Hydrothermal synthesis of polycrystalline BaTiO_3 involves dissolution of barium hydroxide and titanium dioxide in a basic aqueous solvent followed by application of heat (200–500°C) and pressure (160–1300 atm) in a closed vessel for durations of 24–125 h.^{2,10} Although very small particle sizes can be obtained by this technique, stoichiometry is affected by the type and amount of solvent used and can be difficult to control. The cost of these powders is, therefore, comparatively high due to the long incubation periods which limit throughput in small scale production. However, these disadvantages would virtually disappear with large scale chemical synthesis to which the hydrothermal technique is particularly well adapted, as for example in the production of synthetic zeolites.

The size distribution and agglomerate structure of the starting powders exercise an important influence on the microstructures achieved in BaTiO_3 . Hard agglomerates must usually be eliminated in favor of softer, smaller and more uniform agglomerate sizes in order to achieve uniform, homogeneous microstructures.^{11,12} Discontinuous grain growth, which features the growth of large, isolated and generally twinned grains in a matrix of fine grains, is common in titanate ceramics. Although high densities often accompany these

microstructures, the bimodal distribution of grain sizes results in nonreproducibility of the dielectric properties at small ac fields, below the Curie temperature.¹³⁻¹⁵ The dielectric properties of sintered BaTiO_3 , in fact, exhibit a strong dependence on grain size. For grain sizes $\leq 1 \mu\text{m}$, anomalously high room temperature permittivity values are obtained along with a general broadening and flattening of the permittivity peak at the Curie temperature.¹⁴ This has been attributed to the absence of 90° twinning within these grains, giving rise to internal stresses and increased polarization at equivalent applied field.¹⁶ The degree of 90° twinning increases with grain size and results in decreased room temperature permittivity and the enhancement of the permittivity peak at the Curie point.

Impurity effects can also significantly affect both sintering behavior and properties. When present, Al_2O_3 and SiO_2 impurities can contribute to liquid phase formation in the grain boundaries and enhanced densification at the sintering temperature. However, such nonstoichiometric boundaries represent an electrically charged layer¹⁷ which influences grain growth and dielectric behavior, especially since Al can act as an electron acceptor in BaTiO_3 .

The Ba:Ti ratio is another factor which has been shown to dramatically influence microstructural development in high purity BaTiO_3 . Excess BaO typically inhibits grain growth while excess TiO_2 enhances grain growth.¹⁸ In a study involving small excess of Ba or TiO_2 ($0.995 < \text{Ba:Ti} < 1.005$), Sharma et al.¹⁹ reported a solubility limit of $< 0.1 \text{ mol\% TiO}_2$ in BaTiO_3 with increased TiO_2 resulting in formation of a $\text{Ba}_6\text{Ti}_{17}\text{O}_{40}$ second phase.²⁰ Further increase in the Ba:Ti ratio gave rise to increased closed porosity, changes in grain texture, significantly finer grain sizes and precipitation of the barium orthotitanate (Ba_2TiO_4) phase.^{21,22}

From the referenced work, it is evident that chemical preparation methods significantly influence the purity, stoichiometry, particle size and surface

characteristics of the BaTiO_3 powders produced.^{1,3,9,23} These factors, in turn, strongly influence the behavior of the powders during processing and also determine the resultant microstructures and dielectric properties of the sintered ceramic.²⁴ The object of this study, therefore, was to characterize and compare commercially available BaTiO_3 powders prepared by different techniques in order to establish the degree of interchangeability of the powders.

II. Experimental

The BaTiO_3 powders used in this study were commercially available materials which had been prepared by conventional calcination of oxides, by thermal decomposition of oxalates and by hydrothermal synthesis. As-received lots of mixed oxide and oxalate-derived powders had Ba:Ti ratios of 0.997 and 1.002; a stoichiometric mixture of each was obtained by combining appropriate amounts of like powders within these ratios. The hydrothermally prepared powder had a Ba:Ti ratio of 0.987.

The powders were characterized in terms of morphology, chemical purity, surface area, particle size and crystallite structure. Morphology of the as-received powders was determined with a [ISI DS-130] Scanning Electron Microscope. Crystallite sizes, lattice parameters and phase purity were evaluated using a [Philips Norelco] diffractometer with filtered $\text{Cu-K}\alpha$ radiation at 25 kV and 10 mA filament current, at a scan rate of $1-4^\circ 2\theta/\text{min}$. Surface areas were measured by a single point BET N_2 adsorption technique using a [Quantachrome Corp., Monosorb] Surface Area Analyzer. Powders were further analyzed by optical emission spectroscopy, wet chemical analysis [Coors Spectro-Chemical Laboratory] and x-ray fluorescence techniques to determine impurity content and Ba:Ti ratios.

Processing of the powders involved wet milling for 4-12 h in polyethylene jars using ZrO_2 media. A solution of 60/40 vol% isopropanol/water was found to

be an effective milling medium with ≈ 1 wt% (Menhaden) fish oil as dispersant. A binder solution, consisting of 1 wt% polyvinyl alcohol (PVA) and 1 wt% Carbowax 4000 in water, was then added to the milled slurry and dispersed for an additional 1.5 h. The slurries were spray-dried using a (Büchi 190) laboratory spray drier and pellets 1.6 cm dia. and ≈ 0.3 cm thick were uniaxially pressed at 172 MPa. The pellets were sintered at 1300–1320°C/1–2 h in air on ZrO_2 setters and were cooled to 1000°C at 50°C/min followed by natural furnace cooling to room temperature.

Densities of pressed and sintered compacts were measured geometrically and by water immersion technique, respectively. SEM analyses were carried out on the pressed and sintered pellets with the grain sizes determined by a line-intercept technique. Dielectric constant and dissipation factor were measured using a capacitance bridge at different frequencies. Measurements were also made under DC bias field to compare changes in capacitance and dissipation factor under bias conditions.²⁵

III. Results and Discussion

Chemical impurities and stoichiometric ratios determined for the powders used are listed in Table 2 while Table 3 compares the surface area, crystallite sizes, particle size, x-ray diffraction and other pertinent data on the characteristics of the as-received powders. The main impurities present in the powders were Al_2O_3 and SiO_2 , at somewhat higher concentration in the oxalate and lowest in the hydrothermal sample. Impurity levels were not significantly different for powders of different stoichiometric ratios. All samples contained SrO (≤ 0.05 wt%), but this is soluble in the BaTiO_3 lattice and effects on the dielectric properties are predictable.

Stoichiometric (Ba:Ti) ratios for the calcined and oxalate powders (Table 2) were in the range of 0.997 to 1.002 and for the hydrothermal powder

the ratio was 0.987 with no excess TiO_2 detected as a second phase. As shown in Table 3, crystallite sizes for the powders ranged from ≈ 16.0 – 26.0 nm and surface areas from 2.3 – 35 m^2/g , in line with the average particle size values which ranged from ≈ 0.7 μm for the hydrothermal to ≈ 1.50 μm for the calcined powder. Unit cell lattice parameters, determined from x-ray diffraction analysis, and calculated theoretical densities are also given in Table 3 for the three powders, and agree with reported values for BaTiO_3 .^{8,24,26}

Figure 1 shows SEM photomicrographs (12kX) of the three starting powders (Ti excess) after dispersion by ball milling in the 60/40 alcohol/water medium, as described. Distinct differences can be observed in the morphology, agglomerate size and structure of the powders. Average agglomerate size for the calcined powder was ≈ 1.5 μm compared with ≈ 0.7 μm for the oxalate and ≈ 0.9 μm for the hydrothermal powder. However, the agglomerate size distribution for the calcined powder (Figure 1a) was relatively wide, in contrast to the more narrowly distributed oxalate powder (Figure 1b). Agglomerate size distribution was intermediate for the hydrothermal powder (Figure 1c) and appeared to be bimodal, but a distinct subagglomerate structure was also evident. Details of this subagglomerate structure are compared for the different powders in the higher magnification SEM photomicrographs (75kX) in Figure 2. The average crystallite sizes determined from Figure 2 are given in Table 3. As seen, the calcined agglomerates (Figure 2a) appear more compacted and dense compared to the oxalate and hydrothermal powders (Figure 2b, 2c) in which the discrete crystallites comprising the subagglomerate structure can be clearly distinguished. This would imply the existence of softer agglomerates in the oxalate and hydrothermal powders which, according to Reed et al.¹¹ can be considered as held together mainly by van der Waals bonding. In contrast, chemical (diffusion) bonding is believed to predominate in the hard, denser agglomerates²⁷ (Figure 2a). The difference noted above was similar for powders

of different stoichiometric ratios, hence powder synthesis was the dominant influence noted in shaping the morphology, particle size, agglomerate and subagglomerate structure of the different starting powders.

Table 4 compares data for pressed density, fired density, linear shrinkage and average bimodal grain size for the different powders and stoichiometric (Ba:Ti) ratios. Differences between the calcined and oxalate samples could be attributed mainly to the smaller size and higher reactivity of the oxalate powders. For powders of equivalent stoichiometry, this resulted in lower pressed but higher fired density and shrinkage for the latter. The hydrothermal powder, because of its much smaller particle size and different agglomerate characteristics, gave significantly lower pressed density but higher shrinkage and fired density. Stoichiometric effects within powder types (calcined or oxalate) on the pressed density was negligible. Differences were mainly exhibited in decreasing density and grain size with increasing Ba:Ti ratio, with expected influences on the defect states.²⁸

The effect of powder characteristics on the grain size and sintered microstructures is illustrated in Figures 3 and 4 for the oxalate powders and in Figures 5 and 6 for the calcined and hydrothermal powders, respectively. For all the powders, the presence of discontinuous grain growth within a fine-grained matrix was the dominant characteristic of the microstructures.^{18,29}

Figure 3 compares the effect of stoichiometry on discontinuous grain growth behavior for the 0.997 and 1.002 Ba:Ti ratio oxalate powders. The presence of excess BaO (Figure 3b) was observed to substantially retard discontinuous grain growth,²² as is evident from the grain size distribution in the SEM photomicrographs of the "as fired" surfaces. Distribution of the grain structure when viewed in polished cross section was similar but of lower contrast. Figures 4a and 4b show details of the large grain structure for the samples in Figure 3 with the fine structures being detailed in Figures 4c and

4d. Interestingly, the fine grained matrix revealed only slight differences between the two samples, both microstructures appearing dense, uniform and similar in grain size. This would suggest that excess Ba inhibits mainly growth of the large grains and might, therefore, be less effective where small, uniform-sized particles are involved.

In contrast to the oxalate powders, the effect of stoichiometry on the calcined powders showed significantly less growth inhibition with excess Ba, as indicated in Figure 5, where the large grain development is seen to be almost complete with only a relatively small volume concentration of small grains remaining. This may be attributed, in part, to the higher firing temperature used ($1320^{\circ}\text{C}/1\text{ h}$) to achieve equivalent densities, but since the observed trends at $1300^{\circ}\text{C}/2\text{ h}$ were similar, it seems evident that the expected stoichiometric effects were suppressed by variations in processing of the initial powders.³⁰

Figure 6 shows the bimodal grain size distribution obtained with the hydrothermal powder. The large grain volume was intermediate between the calcined and oxalate derived powders but grain sizes (both coarse and fine) were smaller. The fine grained matrix was again very uniform. Grain size data are compared in Table 4 for all the samples and show the expected trend of decreasing size with increasing Ba:Ti ratio for both the large and fine grains.

Figure 7 shows the effect of stoichiometry on the grain size and volume percent coarse grain development in the sintered calcined and oxalate samples. Growth rate of the large grains, as can be seen from the microstructures were higher for the calcined samples at equivalent stoichiometry, reflecting the wider particle size distribution in the initial powder. The observed growth rate was slowest in the hydrothermal sample attributable to the larger number of coarse grains per unit volume.

Figure 8 compares dielectric constant behavior as a function of temperature for the three different type powders with excess Ti (Ba:Ti ratio < 1.00). The

data presented reflect the grain size distribution and microstructures described for the different powders. For BaTiO_3 , the increase in Curie peak height and decrease in tetragonal phase permittivity below the Curie temperature with increasing grain size has been attributed to the presence or absence of 90° twinning. In fine grained ($\leq 1\mu\text{m}$) BaTiO_3 , 90° twins are absent, giving rise to internal stress as the ceramic is cooled through the Curie point. The twins which occur in coarse grained BaTiO_3 relieve the stress and result in a ceramic of lower dielectric constant.^{14,16} Thus, for the hydrothermal samples, dielectric constants were lower at 25°C but were sharply peaked at the Curie temperature ($\approx 125^\circ\text{C}$) reflecting the relatively high concentration of coarse grains. The oxalate samples, in contrast, showed higher room temperature dielectric constants but a relatively subdued T_c peak, attributed to the presence of fewer coarse grains.²⁹ The calcined samples gave the lowest dielectric constants in agreement with the very large grains and relative paucity of small grains in the microstructure.³¹

Dielectric constant and dissipation factor data as a function of Ba:Ti ratio for the oxalate samples are given in Figure 9. The tetragonal phase dielectric constant is seen to decrease with increasing Ba:Ti ratio, which corresponded also to a decrease in density and grain size. Dissipation factor losses were similar for all samples except above the Curie point where the loss increased inversely with the grain size and density.²⁹ Figure 10 shows dielectric constant behavior as a function of stoichiometric BaTiO_3 ratio for the calcined powders. The dielectric properties were similar for all three ratios in line with the close similarity of the microstructures. Figure 11 compares the dielectric constant and loss tangent behavior for the hydrothermal samples at 1.0 and 10.0 kHz. Differences within this frequency range were minimal, and this trend was noted also for the oxalate and calcined samples.

Comparison of the oxalate and calcined powders at equivalent stoichiometric

(Ba:Ti) ratios showed agreement with the grain size distribution and trends indicated in Figure 7. Average grain sizes were large and of narrower distribution for the calcined samples as noted, hence the lower sensitivity in dielectric properties with stoichiometric changes. The losses for the three samples followed the expected grain size trends, higher losses being obtained in the samples with the coarser grains.

The effect of dc bias field on the capacitance change (ΔC) as a function of stoichiometry is shown in Figures 12a and 12b for the different samples. An initial increase in capacitance for the calcined samples (Figure 12a) can be attributed to increased polarization caused by domain rotation within the large grains, since this behavior was not observed in any of the samples with average grain size less than $\approx 25 \mu\text{m}$. The decrease in incremental capacitance with excess Ba content supports this view, since the presence of the large Ba^{2+} ions as a grain boundary phase would tend to reduce grain size and twinning and also to increase the pore phase,²² all deleterious to easy domain rotation. Each sample showed a non-linear decrease in capacitance at bias fields greater than $\approx 80 \text{ V/cm}$. This non-linearity has been explained in terms of an inducement of non-ferroelectric states in the ferroelectric grains as a result of the bias field.^{24,32} Since the smaller grain sizes would be more resistant to this phenomenon, reversal of the capacitance decrease at the higher fields again takes place in the excess Ba samples. The smaller capacitance change with bias field for the hydrothermal sample can plausibly be attributed to the higher concentration of small grains.

Changes in dissipation factor with dc bias field for the different sintered samples at 100 kHz are shown in Figure 13. Dissipation losses generally increased with bias field, attributed to increased dc conduction and polarization in the samples. Losses also increased with grain size (excess TiO_2) and density but the range in the calcined samples was narrower, reflecting

the narrower grain size distribution in these samples. This behavior can be explained in terms of the expected higher grain boundary phase and hence higher insulation resistance for the smaller grain size samples, aided also by the small distributed porosity.³³ The hydrothermal samples showed the lowest dissipation loss behavior, again reflecting the smaller grain size and higher grain boundary phase.

IV. Conclusions

1. Synthesis method and precursor origin were found to be the dominant influences on morphology, particle size, surface area, agglomerate and sub-agglomerate structure in the commercial high purity BaTiO_3 powders studied.
2. The differences in powder characteristics resulted in significant variation in microstructure, density, grain size distribution and dielectric properties of the sintered BaTiO_3 samples.
3. Stoichiometry (Ba:Ti ratio) was also found to significantly influence grain size development, porosity and dielectric properties, in agreement with previous observations.
4. In view of the above, interchangeability of powders could not be achieved, hence close control of all phases of powder preparation is indicated in order to obtain reproducible microstructures in sintered BaTiO_3 .

V. Acknowledgements

This work was supported by the Office of Naval Research under contract No. N-00014-80-K-0969 and in part by the Material Science Foundation under MRL Grant DMR 80-20250.

VI. References

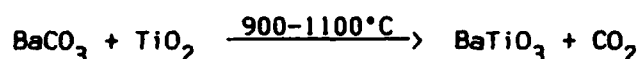
1. P. K. Gallagher and J. Thompson, Jr., "Thermal Analysis of Some Barium and Strontium Titanyl Oxalates," J. Am. Ceram. Soc., **48** [12] 644-47 (1965).
2. A. N. Christensen, "Hydrothermal Preparation of Barium Titanate by Transport Reactions," Acta Chem. Scand., **24** [7] 2447-52 (1970).
3. K. S. Mazdidasni, "Fine Particle Perovskite Processing," Bull. Am. Ceram. Soc., **63** [4] 591-94 (1984).
4. Y. Ozaki, "Ultrafine Electroceramic Powder Preparation from Metal Alkoxides," Ferroelectrics, **49**, 285-96 (1983).
5. T. A. Wheat, "Techniques for Producing Reactive and Homogeneous Ceramic Powders," J. Can. Ceram. Soc., **46** 11-18 (1977).
6. K. Iizumi, K. Sobata and K. Kudaka, "Thermal Decomposition of Barium Titanate (IV) bis (Oxalate) Oxide and the Formation of Barium Titanate," Yogyo Kyokai-Shi, **92** [1] 4-9 (1984) [Japan].
7. P. K. Gallagher and F. Schrey, "Thermal Decomposition of Some Substituted Barium Oxalates and Its Effect on the Semiconducting Properties of the Doped Materials," J. Am. Ceram. Soc., **46** [12] 567-73 (1963).
8. K. Kiss, J. Madger, M. S. Vukasovich and R. J. Lockhart, "Ferroelectrics of Ultrafine Particle Size: I. Synthesis of Titanate Powders of Ultrafine Particle Size," J. Am. Ceram. Soc., **49** [6] 291-95 (1966).
9. Y. Enomoto and A. Yamaji, "Preparation of Uniformly Small-Grained BaTiO_3 ," Bull. Am. Ceram. Soc., **60** [5] 566-70 (1981).
10. L. I. Shvets, N. A. Ovramenko and F. D. Ovramenko, "Hydrothermal Synthesis of Highly-Dispersed Barium Titanate," Dokl. Akad. Nauk SSSR **284** [4] 889-91 (1979).
11. J. S. Reed, T. Carbone, C. Scott and S. Lukasiewicz, "Some Effects of Aggregates and Agglomerates in the Fabrication of Fine-Grained Ceramics," Processing of Crystalline Ceramics, Ed. H. Palmour, R. F. Davis and T. M. Hare, 171-80, (1978).

12. D. E. Niesz and R. B. Bennett, "Structure and Properties of Agglomerates," Ceramic Processing Before Firing, Ed. G. Y. Onoda, Jr. and L. L. Hench, John Wiley and Sons, New York, 61-74, (1978).
13. M. P. Harmer, Y. H. Hu, M. Lal and D. M. Smyth, "The Effects of Composition and Microstructure on Electrical Degradation in BaTiO_3 ," Ferroelectrics, **49**, 71-74 (1983).
14. C. A. Miller, "Hysteresis Loss and Dielectric Constant in Barium Titanate," Brit. J. Appl. Phys., **18** 1689-97 (1967).
15. W. Heywang, "Structural Engineering of Ferroelectrics," Ferroelectrics, **49** 3-14 (1983).
16. W. R. Buessem, L. E. Cross, and A. K. Goswami, "Phenomenological Theory of High Permittivity in Fine-Grained Barium Titanate," J. Am. Ceram. Soc., **49** [1] 33-36 (1966).
17. P. F. Bongers and P. E. C. Franken, "Secondary Phases and Segregation Layers at Grain Boundaries in Electronic Ceramic Materials," Grain Boundary Phenomena in Electronic Ceramics, Vol. 1, ed. by L. M. Levinson, The Am. Ceram. Soc., Inc., Columbus, OH, pp. 38-52 (1981).
18. F. Kulcsar, "A Microstructure Study of Barium Titanate Ceramics," J. Am. Ceram. Soc., **39** [1] 13-17 (1956).
19. R. K. Sharma, N. H. Chan, and D. M. Smyth, "Solubility of TiO_2 in BaTiO_3 ," J. Am. Ceram. Soc., **64** [8] 448-51 (1981).
20. H. M. O'Bryan, Jr., and J. Thompson, Jr., "Phase Equilibria in the TiO_2 -Rich Region of the System BaO-TiO_2 ," J. Am. Ceram. Soc., **57** [12] 522-26 (1974).
21. N. K. Chan, R. K. Sharma, and D. M. Smyth, "Nonstoichiometry in Undoped BaTiO_3 ," J. Am. Ceram. Soc., **64** [9] 556-62 (1981).
22. A. Beauger, J. C. Mutin and J. C. Niepce, "Role and Behaviour of Orthotitanate BaTiO_4 During the Processing of BaTiO_3 Based Ferroelectric Ceramics," J. Mater. Sci., **19** 195-201 (1984).

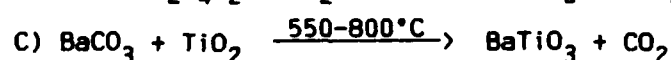
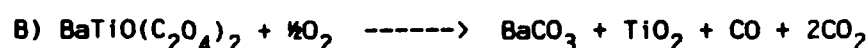
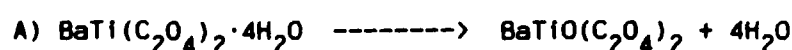
23. J. J. Rosenthal and S. D. Stoddard, "A Study of Process Variables in Barium Titanate Ceramics," Bull. Am. Ceram. Soc., **37** [8] 370-75 (1958).
24. K. S. Mazdiyasni and L. M. Brown, "Microstructure and Electrical Properties of Sc_2O_3 -Doped, Rare-Earth-Oxide-Doped and Undoped BaTiO_3 ," J. Am. Ceram. Soc., **4** [11] 539-43 (1971).
25. H. Diamond, "Variation of Permittivity with Electric Field in Perovskite-Like Ferroelectrics," J. Appl. Phys., **32** [5] 909-15 (1961).
26. L. K. Templeton and J. A. Pask, "Formation of BaTiO_3 from BaCO_3 and TiO_2 in Air and in CO_2 ," J. Am. Ceram. Soc., **42** [5] 212-16 (1959).
27. H. Rumpf and H. Schubert, "Adhesion Forces in Agglomeration Processes," Ceramic Processing Before Firing, Ed. G. Y. Onoda, Jr. and L. L. Hench, John Wiley and Sons, New York, 357-78, (1978).
28. J. F. Baumard, P. Abelard and D. M. Smyth, "A Representation of the Defect Structure of Pure Barium Titanate," Rev. Int. Hautes Temp. Refract. **20** 3-16 (1983)[Fr].
29. E. P. Hyatt, S. A. Long and R. E. Rose, "Sintering High Purity BaTiO_3 ," Bull. Am. Ceram. Soc., **46** [8] 732-36 (1967).
30. Aléna K. Maurice, "Powder Synthesis, Stoichiometry and Processing Effects on Properties of High Purity Barium Titanate," M.S. Thesis, University of Illinois, Department of Ceramic Engineering, Urbana, IL. 1984.
31. K. Yamashita, S. Yamazaki, K. Koumoto and H. Yanagida, "Numerical Estimation of the Dependence of Dielectric Constant of BaTiO_3 Thick Films on Grain Size Distribution," Jap. J. Appl. Phys., **20** [10] 1833-40 (1981).
32. W. Heywang, "Semiconducting Barium Titanate," J. Mater. Sci. **6** 1214-1226 (1971).
33. G. J. Hill, "Energy Storage in High-Permittivity Ceramics: Survey of Materials Based Upon Barium Titanate," Proc. Brit. Ceram. Soc. [18] 201-20 (1970).

Table 1
BaTiO₃ Preparation Methods

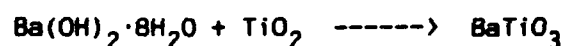
1. Calcination of Carbonate and Oxide



2. Oxalate Precursors



3. Hydrothermal Synthesis



(200-500°C; 160-1300 atm; 60-125h; pH>7)

4. Alkoxide Precursors

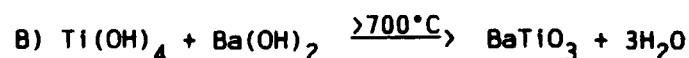
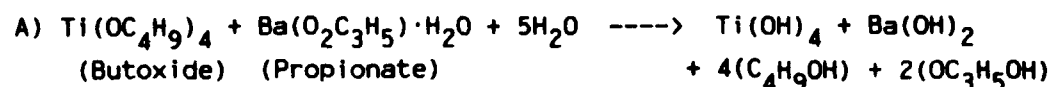


Table 2
Typical Lot Analysis for BaTiO₃ Powders*

<u>Constituents</u>	<u>Calcined</u> (wt %)	<u>Oxalate</u> (wt %)	<u>Hydrothermal</u> (wt %)
BaO	65.37	65.56	62.57
TiO ₂	34.25	34.25	34.25
SrO	0.02	0.01	0.05
ZrO ₂	-	0.01	0.02
SiO ₂	0.01	0.05	0.01
Al ₂ O ₃	0.02	0.08	0.01
Fe ₂ O ₃	-	0.03	0.004
Nb ₂ O ₅	-	0.01	0.003
NaO ₂	0.004	0.001	0.001
Mol Ratio	0.997	0.997	0.987
LOI	0.18%	0.22%	4.00%

*TAM Ceramics, Inc., Niagra Falls, New York 14305

Table 3
Characterization of BaTiO₃ Powders

<u>Properties</u>	<u>Calcined</u>		<u>Oxalate</u>		<u>Hydrothermal</u>
Ba:Ti	0.997	1.002	0.997	1.002	0.987
a _o , nm	0.4002	0.3982	0.4011	0.4012	0.4019
c _o , nm	0.4047	0.4025	0.4033	0.4024	0.4040
c/a	1.011	1.011	1.006	1.003	1.005
D _x , g/cm ³	5.964	6.074	5.957	5.986	5.884
Avg. Xtl. Size, nm					
XRD	24.9	24.9	25.5	25.7	22.6
SEM	≈22.5	≈23.0	≈20.0	≈21.0	≈16.5
Avg. PS, μm	1.50	1.45	0.96	0.91	0.68
SA, m ² /g (BET)	2.30	2.36	3.52	3.40	34.5

Table 4
Comparison of BaTiO₃ Powders Prepared by Different Techniques

<u>Sample</u>	<u>Pressed Density</u>	<u>Fired Density</u>	<u>Linear Shrink.</u>	<u>Avg. Grain Size</u>	
(Ba:Ti)	(%ThD) *	(%ThD) *	(%) **	Fine	Coarse
				(μm)	
0.997 oxa	59.2	98.0	16.4	1.00	32.0
1.000 oxa	59.0	97.6	16.2	0.95	27.2
1.002 oxa	59.9	97.0	16.0	0.89	22.1
0.997 cal	61.4	95.6	14.6	3.9	36.0
1.000 cal	61.1	96.1	14.8	3.5	33.0
1.002 cal	60.1	96.6	15.5	3.0	29.5
0.987 hyd	44.3	97.9	24.3	0.7	22.1

* Theoretical density as in Table 1

** Milled 12 hours, sintered at 1300°C/1 h

VII. List of Figures

- Figure 1. SEM photomicrographs (12 kX) of BaTiO_3 powders after dispersion (12 h milling) showing agglomerate structure and particle size distribution. A) calcined, B) oxalate, C) hydrothermally derived powders.
- Figure 2. High magnification SEM photomicrographs (75 kX) of samples in Figure 1 showing details of subagglomerate structure.
- Figure 3. SEM photomicrographs of as-fired surface of oxalate derived BaTiO_3 showing effect of stoichiometry on bimodal grain size distribution. A) $\text{Ba}:\text{Ti} = 0.997$, B) $\text{Ba}:\text{Ti} = 1.002$
- Figure 4. SEM photomicrographs of as-fired surface of oxalate derived BaTiO_3 samples ($1300^\circ\text{C}/1\text{ h}$) showing detail of grain structures. A) $\text{Ba}:\text{Ti} = 0.997$, B) $\text{Ba}:\text{Ti} = 1.002$, C) and D) small grain structure for A) and B), respectively
- Figure 5. SEM photomicrographs of as-fired surface of BaTiO_3 calcined samples showing effect of stoichiometry on bimodal grain size distribution ($1320^\circ\text{C}/1\text{ h}$). A) $\text{Ba}:\text{Ti} = 0.997$, B) $\text{Ba}:\text{Ti} = 1.002$
- Figure 6. SEM photomicrographs of hydrothermally derived BaTiO_3 sample showing bimodal grain distribution ($1300^\circ\text{C}/1\text{ h}$). A) as fired surface, B) detail of small grain structure
- Figure 7. Effect of stoichiometry and powder synthesis method on grain size and vol% coarse grains in sintered BaTiO_3 .
- Figure 8. Comparison of dielectric constant behavior with temperature for sintered BaTiO_3 samples of $\text{Ba}:\text{Ti} \approx 0.997$.
- Figure 9. Effect of stoichiometry on dielectric constant and $\tan \delta$ as a function of temperature for oxalate derived BaTiO_3 samples.
- Figure 10. Effect of stoichiometry on dielectric constant and $\tan \delta$ as a function of temperature for calcined BaTiO_3 samples.

Figure 11. Effect of frequency and temperature on dielectric constant and $\tan \delta$ for hydrothermally derived BaTiO_3 sample.

Figure 12. Effect of DC bias and stoichiometry on percent capacitance change of sintered BaTiO_3 samples. A) calcined, B) oxalate and hydrothermally derived precursors.

Figure 13. Effect of DC bias and stoichiometry on dissipation factor of sintered BaTiO_3 samples prepared from calcined, oxalate and hydrothermally derived precursors.

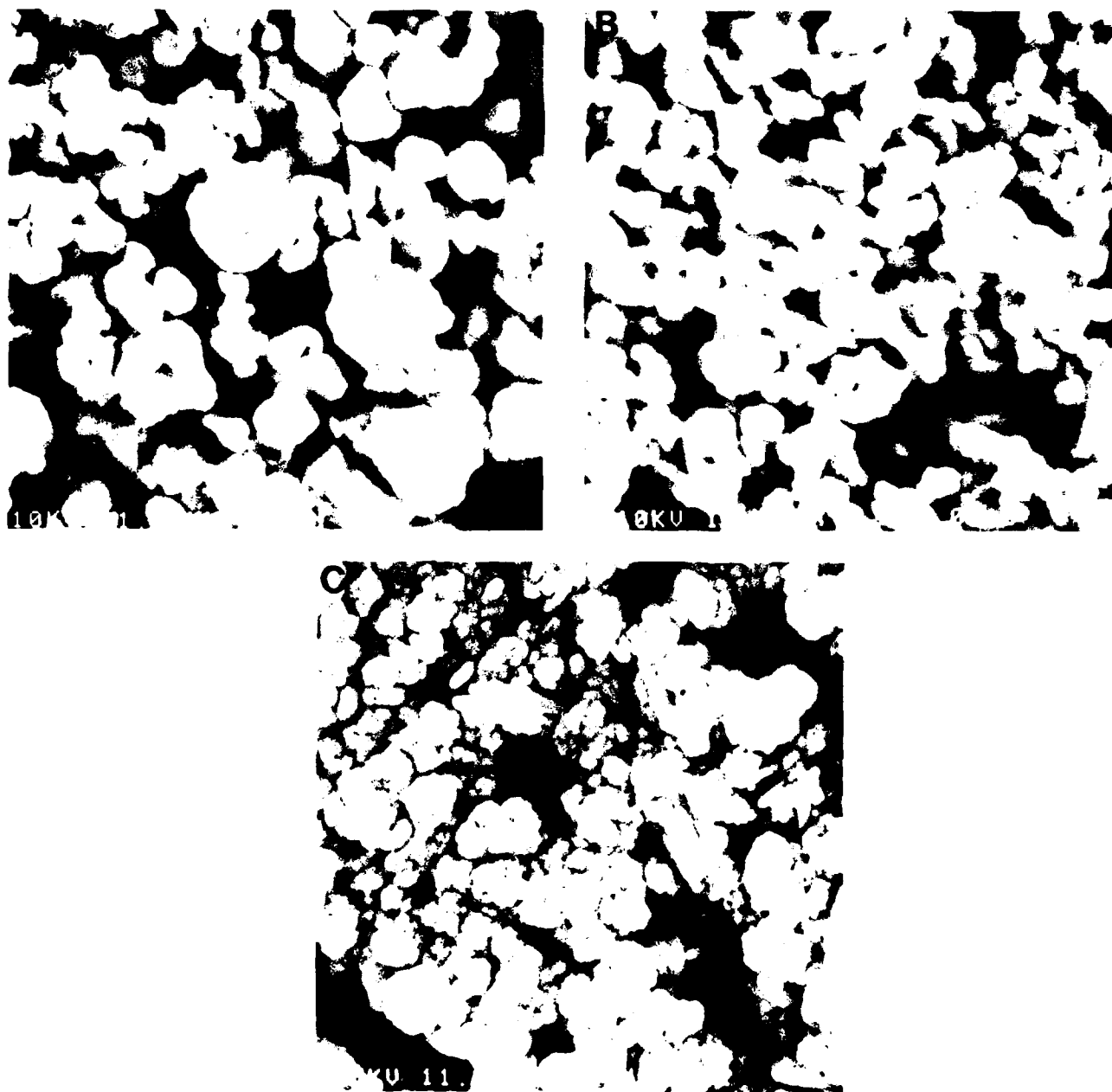


Figure 1. SEM photomicrographs (12 kX) of BaTiO_3 powders after dispersion (12 h milling) showing agglomerate structure and particle size distribution. A) calcined, B) oxalate, C) hydrothermally derived powders.

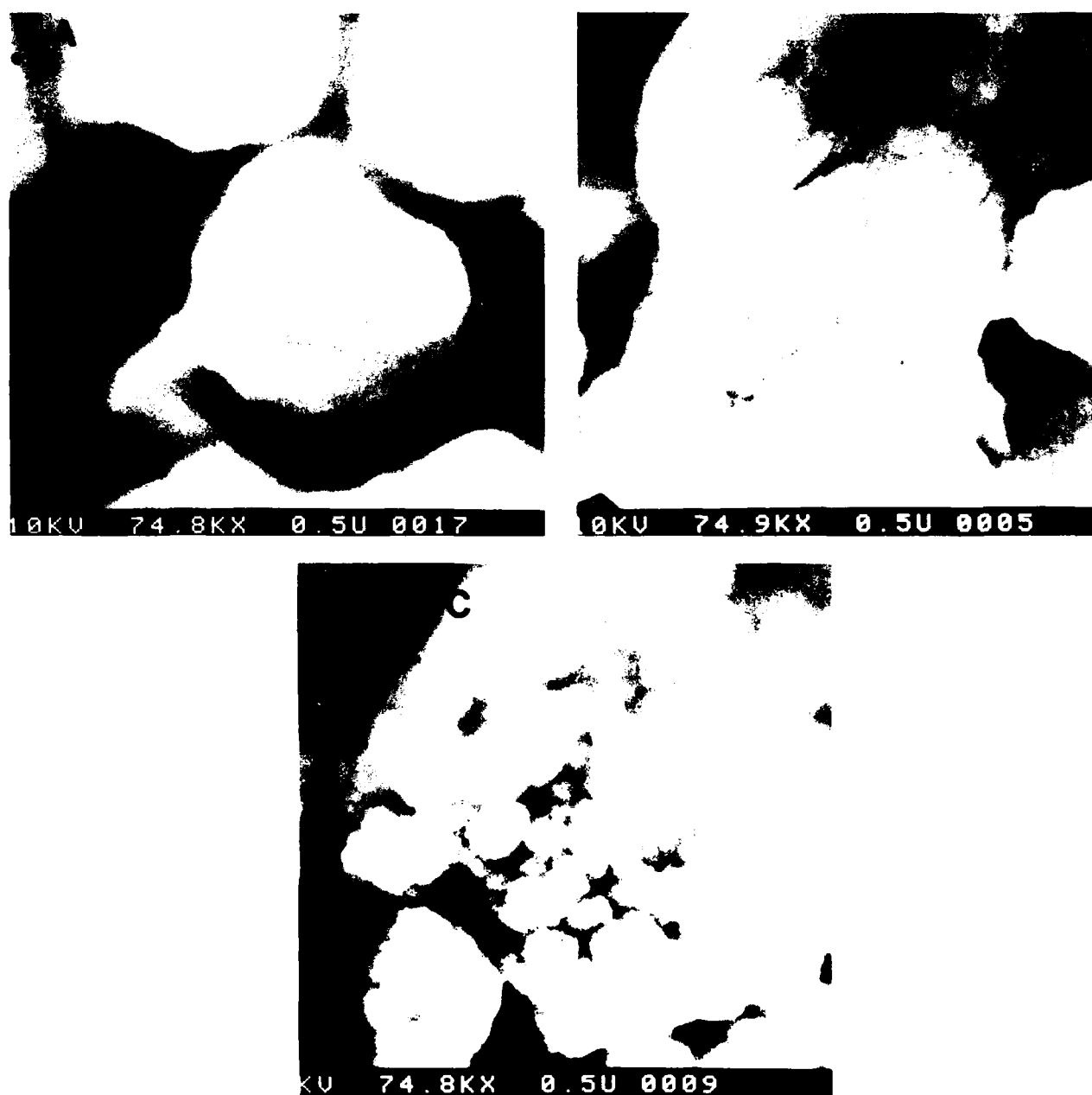


Figure 2. High magnification SEM photomicrographs (75 kX) of samples in Figure 1 showing details of subagglomerate structure.

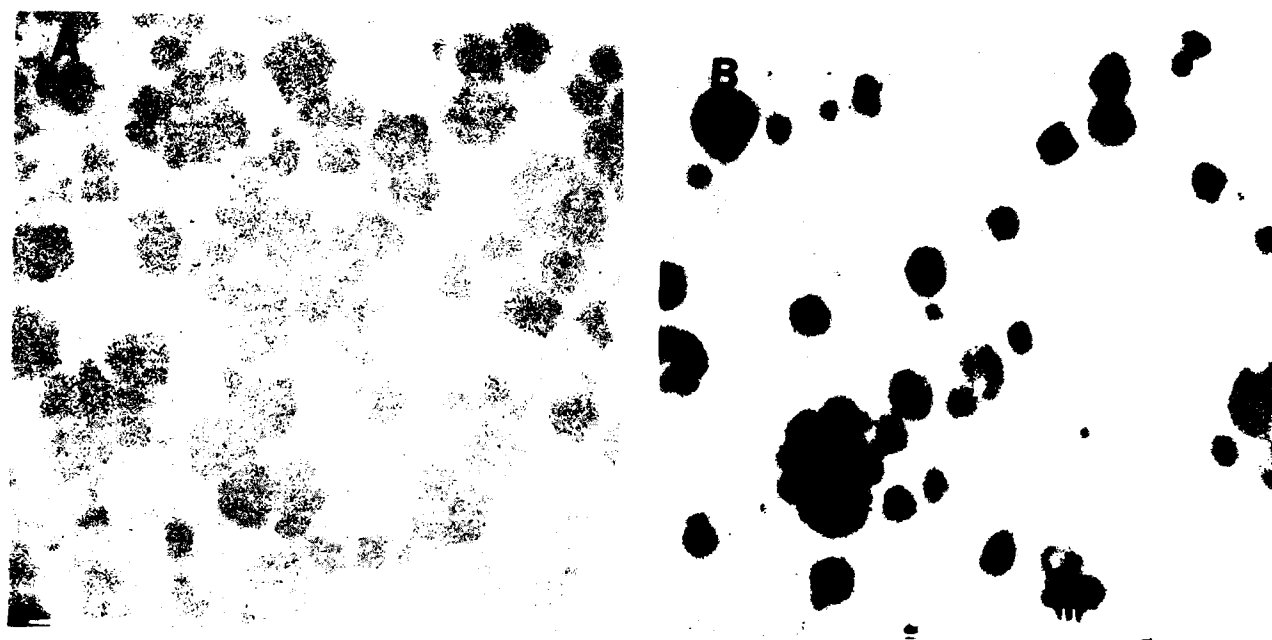


Figure 3. SEM photomicrographs of as-fired surface of oxalate derived BaTiO_3 showing effect of stoichiometry on bimodal grain size distribution. A) $\text{Ba}:\text{Ti} = 0.997$, B) $\text{Ba}:\text{Ti} = 1.002$

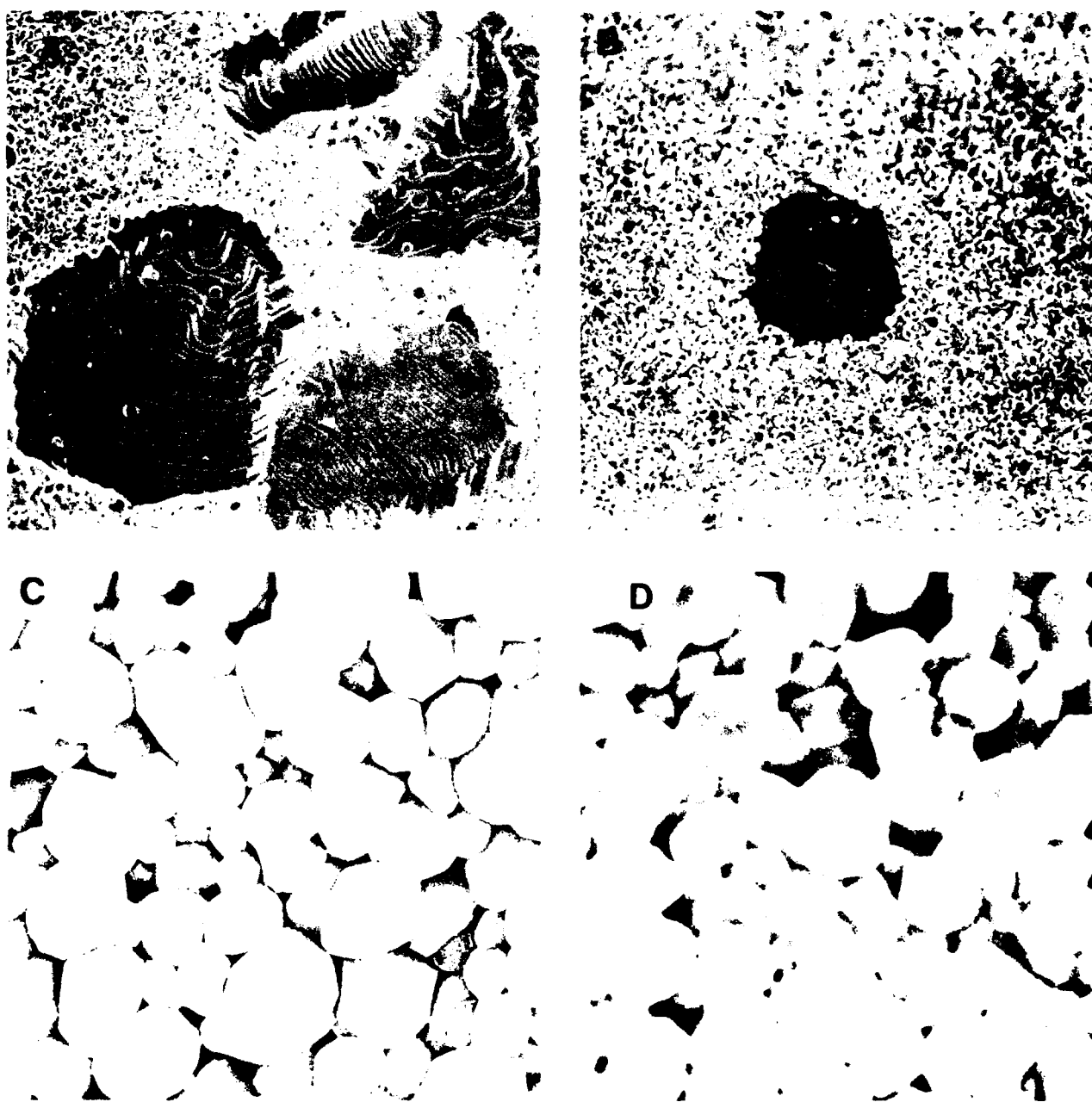


Figure 4. SEM photomicrographs of as-fired surface of oxalate derived BaTiO_3 samples ($1300^\circ\text{C}/1\text{ h}$) showing detail of grain structures. A) $\text{Ba}:\text{Ti} = 0.997$, B) $\text{Ba}:\text{Ti} = 1.002$, C) and D) small grain structure for A) and B), respectively

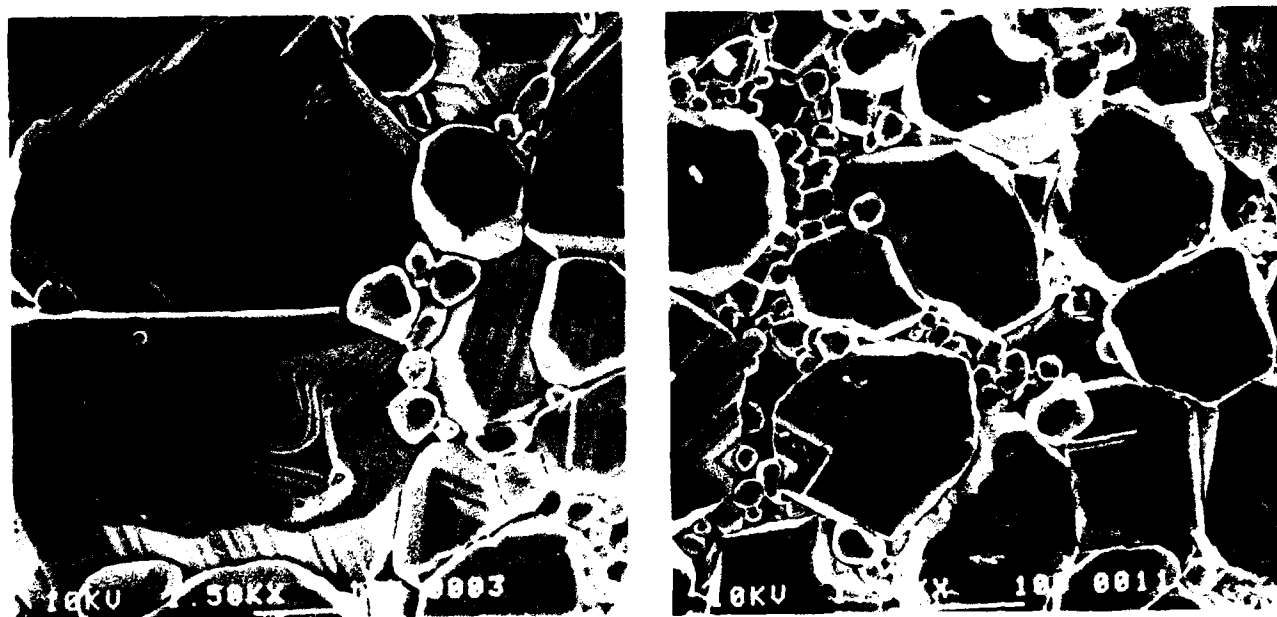


Figure 5. SEM photomicrographs of as-fired surface of BaTiO_3 calcined samples showing effect of stoichiometry on bimodal grain size distribution ($1320^\circ\text{C}/1\text{ h}$). A) $\text{Ba}:\text{Ti} = 0.997$, B) $\text{Ba}:\text{Ti} = 1.002$

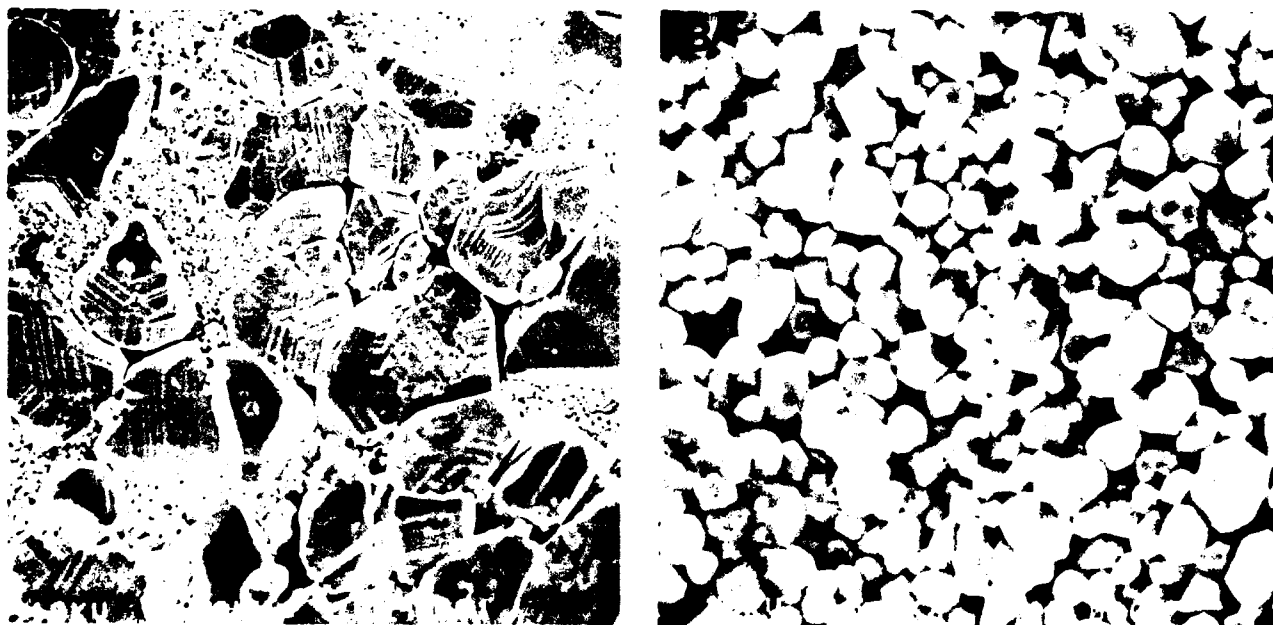


Figure 6. SEM photomicrographs of hydrothermally derived BaTiO_3 sample showing bimodal grain distribution ($1300^\circ\text{C}/1\text{ h}$). A) as fired surface, B) detail of small grain structure

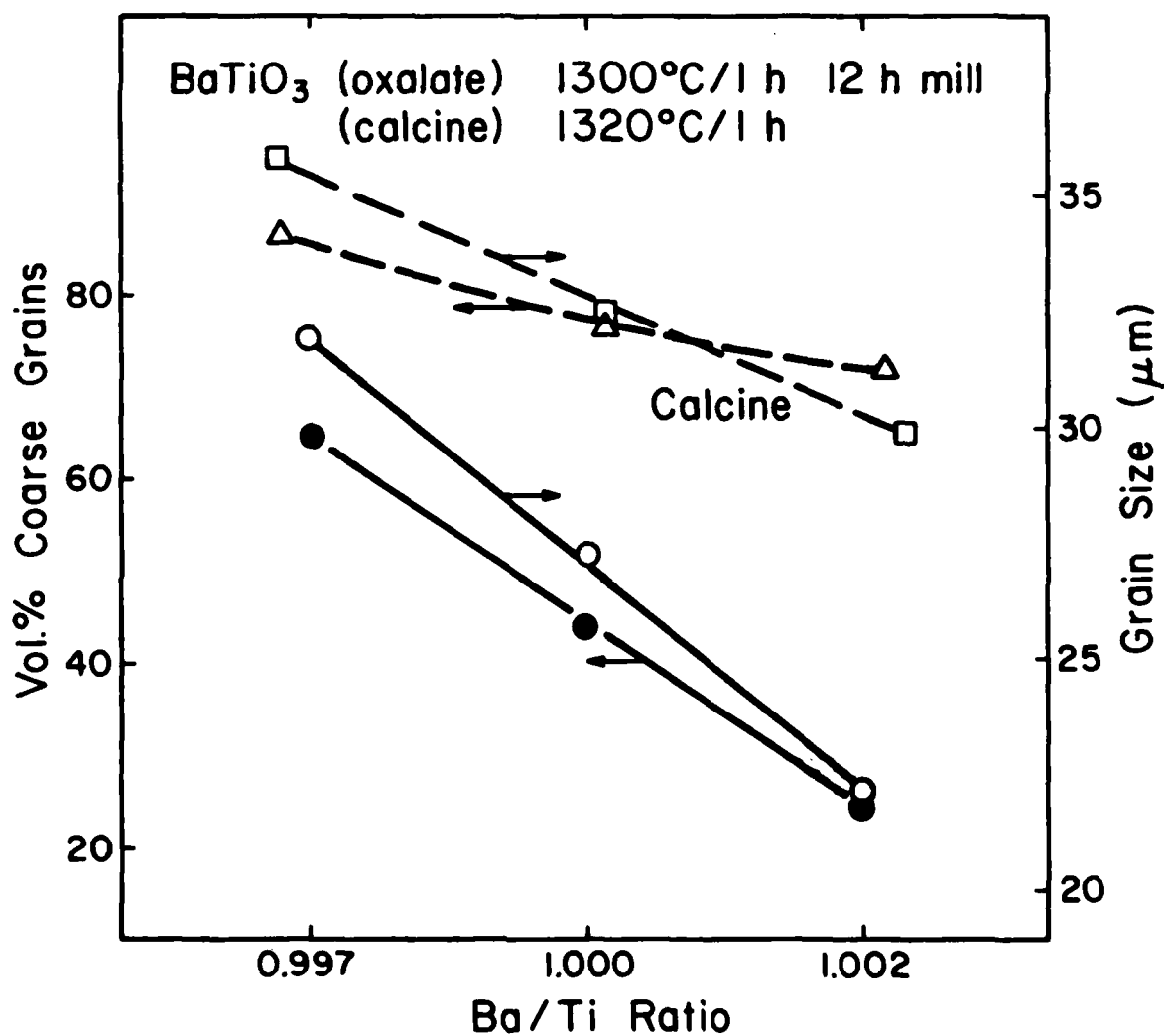


Figure 7. Effect of stoichiometry and powder synthesis method on grain size and vol% coarse grains in sintered BaTiO_3 .

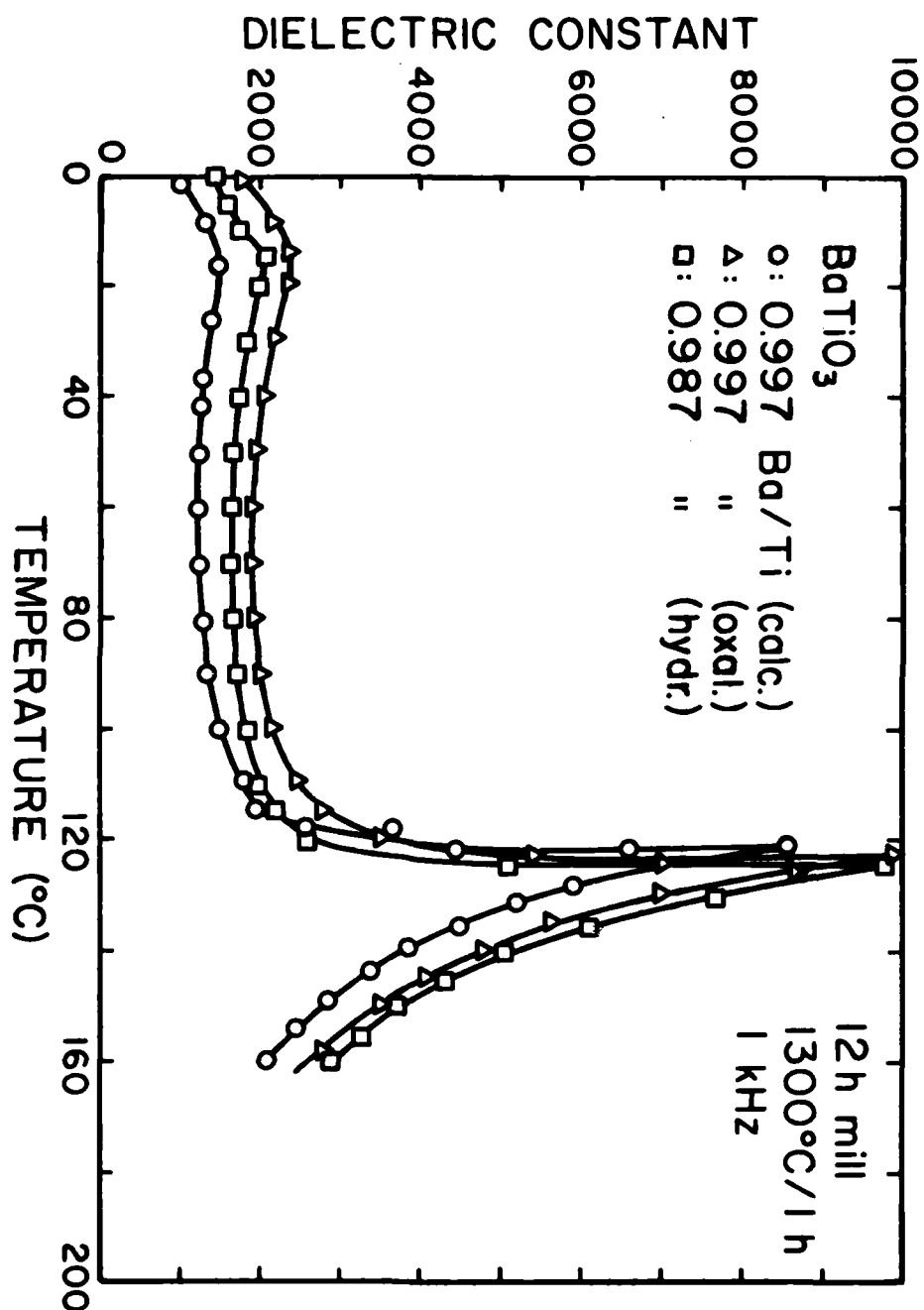


Figure 8. Comparison of dielectric constant behavior with temperature for sintered BaTiO_3 samples of Ba:Ti ≈ 0.997 .

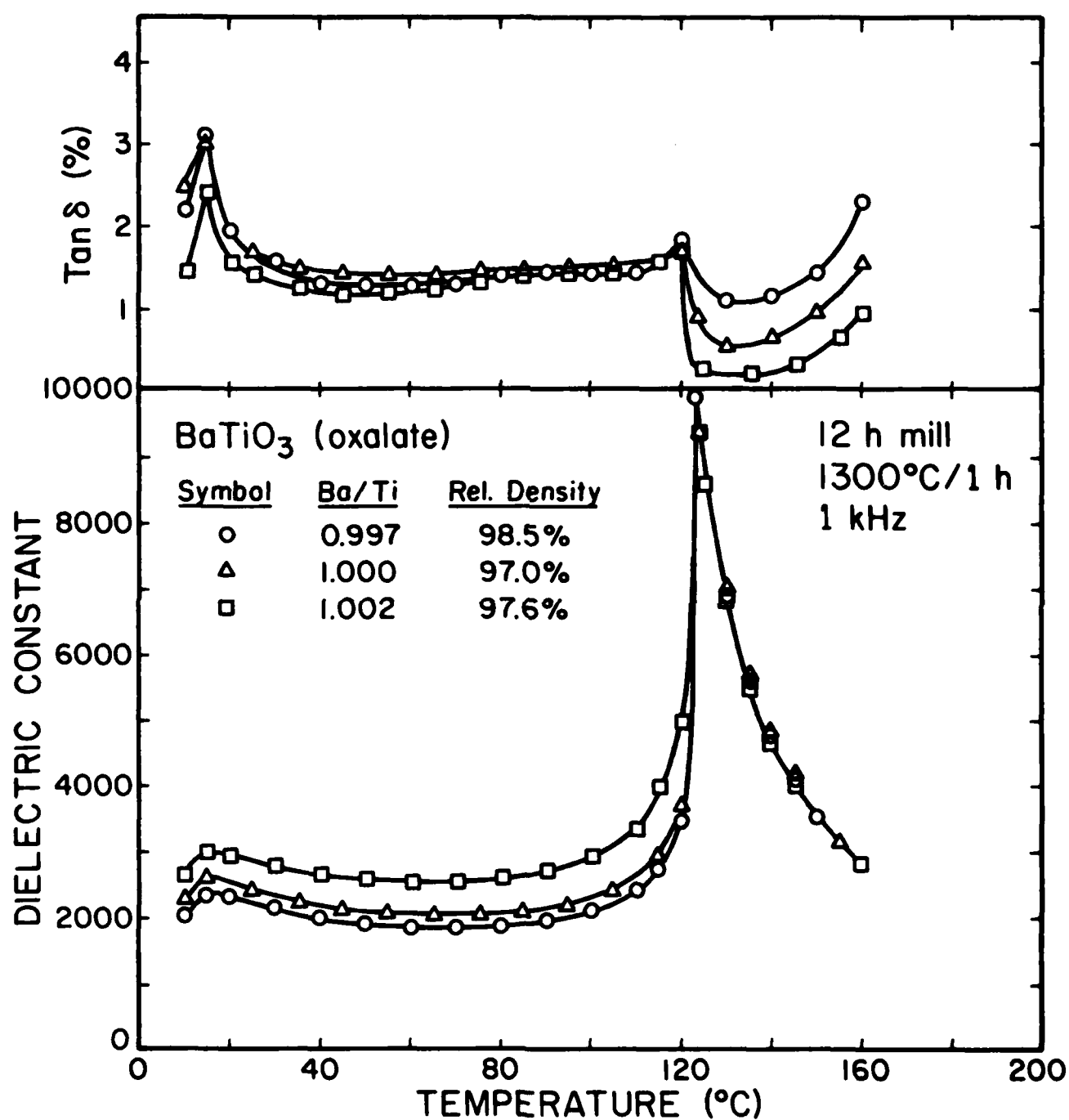


Figure 9. Effect of stoichiometry on dielectric constant and tan δ as a function of temperature for oxalate derived BaTiO₃ samples.

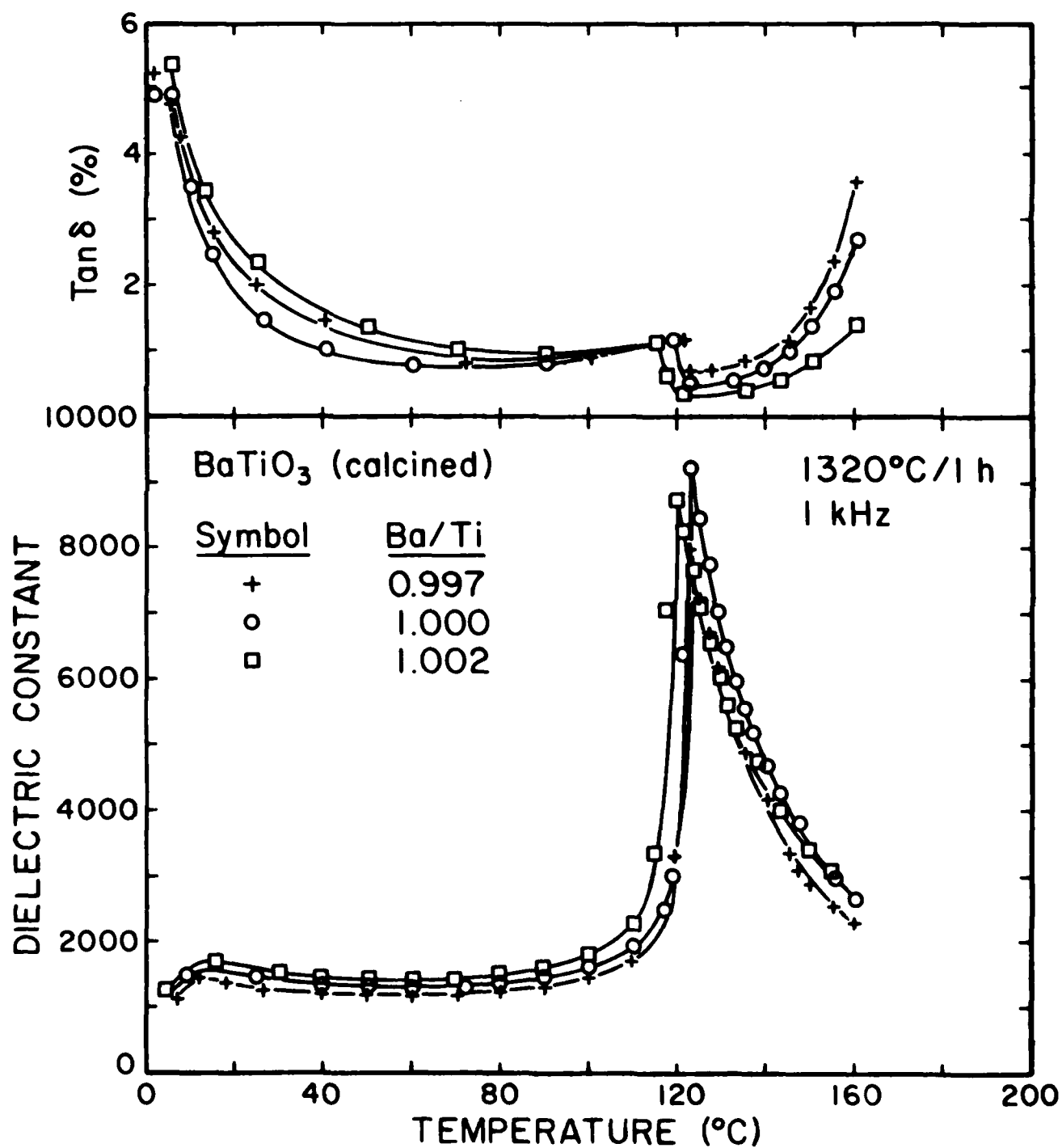


Figure 10. Effect of stoichiometry on dielectric constant and tan δ as a function of temperature for calcined BaTiO_3 samples.

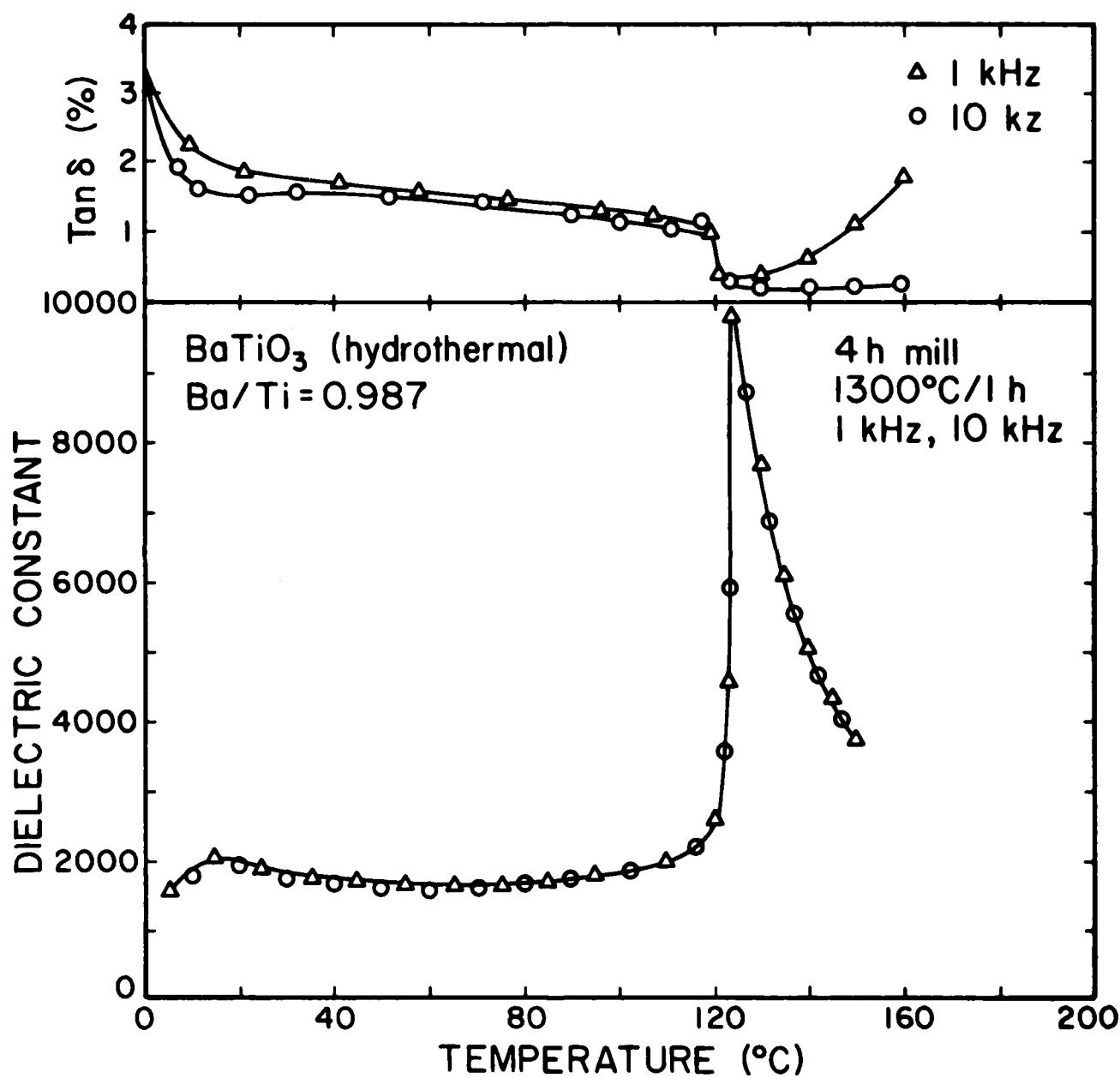


Figure 11. Effect of frequency and temperature on dielectric constant and $\tan \delta$ for hydrothermally derived BaTiO_3 sample.

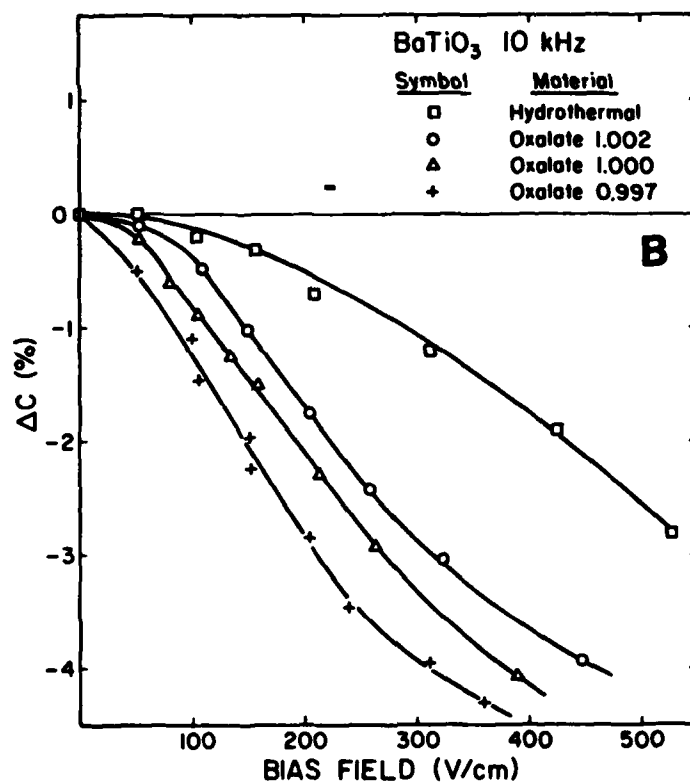
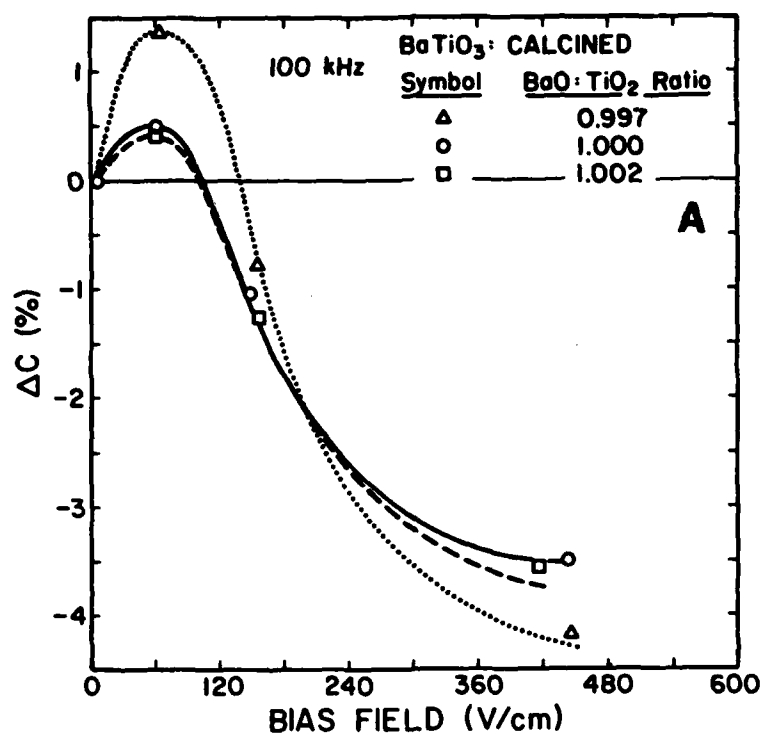


Figure 12. Effect of DC bias and stoichiometry on percent capacitance change of sintered BaTiO₃ samples. A) calcined, B) oxalate and hydrothermally derived precursors.

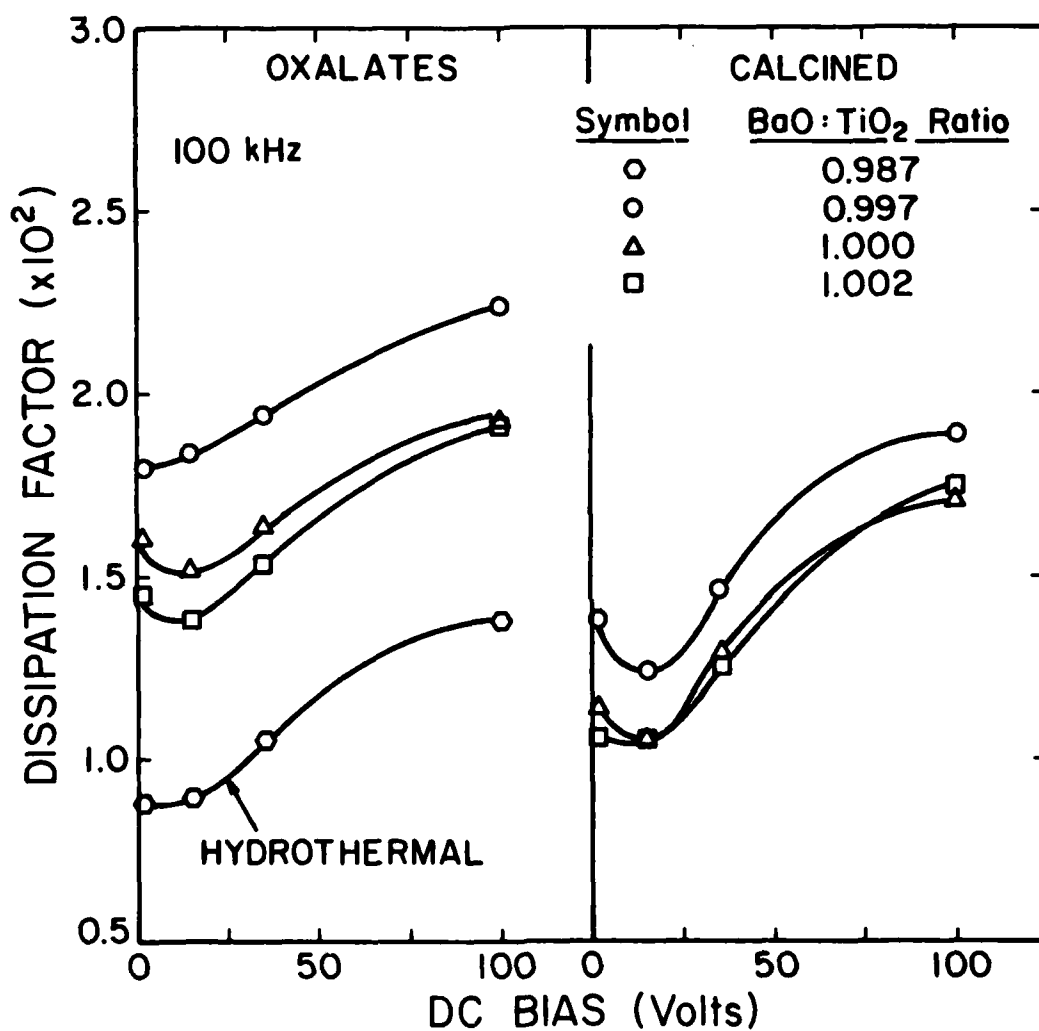


Figure 13. Effect of DC bias and stoichiometry on dissipation factor of sintered BaTiO₃ samples prepared from calcined, oxalate and hydrothermally derived precursors.

Summary of Work Accomplished
Under Contract No. US NAVY-N-00014-80-K-0969

Reports

Reports issued under this contract include the following:

1. R. C. Buchanan and S. Pope, "Optical and Electrical Properties of Yttria Stabilized Zirconia (YSZ) Crystals," (ONR Report #5), University of Illinois at Urbana-Champaign, Department of Ceramic Engineering, Urbana, IL 61801 (September, 1981).
2. R. C. Buchanan and J. Boy, "Effect of Coprecipitation Parameters on Powder Characteristics and On Densification of PZT Ceramics," (ONR Report #6), University of Illinois at Urbana-Champaign, Department of Ceramic Engineering, Urbana, IL (September 1982).
3. R. C. Buchanan and D. M. Wilson, "Densification of Precipitated Yttria Stabilized Zirconia (YSZ) to Achieve Translucent Properties," (ONR Report #7), University of Illinois at Urbana-Champaign, Department of Ceramic Engineering, Urbana, IL (November 1982).
4. R. C. Buchanan and D. M. Wilson, "Role of Al_2O_3 in Sintering of Submicron Yttria Stabilized ZrO_2 Powders," (ONR Report #8), University of Illinois, Department of Ceramic Engineering, Urbana, IL (December 1983).
5. R. C. Buchanan and D. M. Wilson, "Densification of Submicron YSZ Powders with Alumina and Borate Additives," (ONR Report #9), University of Illinois, Department of Ceramic Engineering, Urbana, IL (December 1984).
6. R. C. Buchanan and J. Boy, "Effect of Powder Characteristics on Microstructure and Properties in Alkoxide Prepared PZT Ceramics," (ONR Report #10), University of Illinois, Department of Ceramic Engineering, Urbana, IL (December 1984).
7. R. C. Buchanan and W. W. Davison, "Influence of Alumina on the Structure and Mechanical Properties of Yttria Stabilized Zirconia Composites," (ONR Report #11), University of Illinois, Department of Ceramic Engineering, Urbana, IL (July 1985).
8. R. C. Buchanan and A. K. Maurice, "Preparation and Stoichiometry Effects on Microstructure and Properties of High Purity $BaTiO_3$," (ONR Report #12), University of Illinois, Department of Ceramic Engineering, Urbana, IL (March 1986).
9. R. C. Buchanan and W. W. Davison, "Influence of Al_2O_3 on Properties of Yttria Stabilized Zirconia- Al_2O_3 Composites," (ONR Report #13), University of Illinois, Department of Ceramic Engineering, Urbana, IL (March, 1986).

Theses

1. G. Wolter, "Properties of Hot-Pressed ZrV_2O_7 ," M.S. Thesis, University of Illinois, Department of Ceramic Engineering, Urbana, IL, 1981.
2. H. D. DeFord, "Low Temperature Densification of Zirconium Dioxide with Vanadate Additives," M.S. Thesis, University of Illinois, Department of Ceramic Engineering, Urbana, IL, 1982.
3. J. H. Boy, "Effect of Coprecipitation Parameters on the Powder Characteristics of Lead Zirconate Titanate Prepared for Lead Oxide and Butoxide Precursors," M.S. Thesis, University of Illinois, Department of Ceramic Engineering, Urbana, IL, 1983.
4. R. DiChiara, "Processing and Additive Effects on Densification of Calcia Stabilized Zirconia (YSZ)," M.S. Thesis, University of Illinois, Department of Ceramic Engineering, Urbana, IL, 1983.
5. D. M. Wilson, "Effect of Aluminium and Boron oxides on Densification of Yttria Stabilized Zirconia," M.S. Thesis, University of Illinois, Department of Ceramic Engineering, Urbana, IL, 1984.
6. Aléna K. Maurice, "Powder Synthesis, Stoichiometry and Processing Effects on Properties of High Purity Barium Titanate," M.S. Thesis, University of Illinois, Department of Ceramic Engineering, Urbana, IL, 1984.
7. S. G. Pope, "Development of Electron Beam Interactive Ceramic Films by RF Sputtering for Memory Applications," M.S. Thesis, University of Illinois, Department of Ceramic Engineering, Urbana, IL, 1984.
8. W. W. Davison, "Influence of Alumina on Structural and Mechanical Properties of Yttria-Stabilized Zirconia," M.S. Thesis, University of Illinois, Department of Ceramic Engineering, Urbana, IL, 1985.

Publications

1. D. E. Wittmer and R. C. Buchanan, "Low Temperature Densification of Lead Zirconate Titanate with Vanadium Pentoxide Additive," J. Am. Ceram. Soc., **64** [8] 485-490 (1981).
2. R. C. Buchanan and S. Pope, "Optical and Electrical Properties of Yttria Stabilized Zirconia (YSZ) Crystals," J. Electrochem. Soc., **130**, [4] 962-966 (1982).
3. R. C. Buchanan and J. Boy, "Effect of Coprecipitation Parameters on Powder Characteristics and On Densification of PZT Ceramics," Proc. of U.S. Japan Seminar on Dielectrics and Piezoelectrics, Tokyo, Japan, 1982.
4. A. F. Grandin de l'Eprevier and R. C. Buchanan, "Preparation and Properties of $\text{Ca}_2\text{V}_2\text{O}_7$ Single Crystals," J. Electrochem. Soc., **129** [11] 2562-2565 (1982).
5. A. Sircar and R. C. Buchanan, "Densification of CaO -stabilized ZrO_2 with Borate Additives," J. Am. Ceram., **66** [2] 20-21 (1983).
6. G. Wolter and R. C. Buchanan, "Properties of Hot-Pressed ZrV_2O_7 ," J. Electrochem. Soc., **130** [9] 1905-1910 (1983).
7. R. C. Buchanan, H. D. DeFord, and R. W. Doser, "Effects of Vanadate Phase on Sintering and Properties of Monoclinic ZrO_2 ," Advances in Ceramics, Vol 7, pp. 196-207, in: Additives and Interfaces in Electronic Ceramics, Am. Ceram. Soc., Columbus, OH (1984).
8. R. C. Buchanan and D. M. Wilson, "Role of Al_2O_3 in Sintering of Yttria Stabilized ZrO_2 Powders," Adv. in Ceramics, Vol. 10, pp. 526-540, "Structure and Properties of MgO and Al_2O_3 Ceramics," Editor, W. D. Kingery, Am. Ceram. Society, Columbus, OH (1985).
9. R. C. Buchanan and D. M. Wilson, "Densification of Submicron YSZ Powders with Alumina and Borate Additives," J. Am. Ceram. Soc., 1985 (accepted).
10. R. C. Buchanan and J. Boy, "Effect of Powder Characteristics on Microstructure and Properties in Alkoxide Prepared PZT Ceramics," J. Electrochem. Soc., **132** [7] 1671-1677 (1985).
11. W. W. Davison and R. C. Buchanan, "Influence of Al_2O_3 on Structure and Mechanical Properties of Yttria Stabilized (YSZ)- Al_2O_3 Composites," J. Am. Ceram. Soc., 1985 (accepted).
12. Aléna K. Maurice and R. C. Buchanan, "Processing Effects on Microstructure and Properties of High Purity BaTiO_3 ," J. Am. Ceram. Soc., 1985 (submitted).
13. Aléna K. Maurice and R. C. Buchanan, "Preparation and Stoichiometry Effects on Microstructure and Properties of High Purity BaTiO_3 ," J. Am. Ceram. Soc., 1985 (submitted).

Technical Presentations Made (1985)

1. Mo Bay Chemicals (PEMCO Glass Co.), Baltimore, Md., Jan. 14, 1985, "Composition and Properties of Glasses for Electrical and Electronic Applications," Invited 4 h Lecture-Discussion.
2. IBM Corporation, E. Fishkill, N.Y., Jan. 15, 1985, "Review of Hole Drilling, Dielectric Films and Materials for Packaging Applications," Invited Lecture.
3. American Ceramic Society (Annual Meeting), Cincinnati, Oh., May 5-9, 1985, Three Presentations: 1) Microelectronics Applications of Glasses, 2) Processing Effects on Microstructure and Phase Stability of Tetragonally Stabilized Zirconia (TTZ), 3) Effect of Al_2O_3 on Mechanical Properties and Structure of YSZ- Al_2O_3 Composites.
4. American Society for Engineering Education (ASEE), Atlanta, Ga., Jun 16-18, 1985, "High Technology Ceramics". Invited Lecture.
5. Center for Professional Advancement, E. Brunswick, N.J., Aug. 14-16, 1985, Course Director for "Ceramic Applications in Electronics," Five (2-h) Lectures: a) Electronic Ceramics/Dielectrics Properties, b) Glasses and Substrates in Electronics, c) Thick Film Hybrid Circuits; d) Magnetic Ceramics (Ferrites), e) Processing of Electronic Ceramics.
6. Pennsylvania State University, State College, PA, Oct. 8-9, 1985, ONR Technical Program Review Meeting, "Processing of Dielectric and Structural Ceramics."
7. The First Great Lakes Electron Microscopy Conference, Oakbrook, Il, Oct. 11-13, 1985, "Microstructures of High Purity Barium Titanate as Influenced by Variations in Processing Parameters". (A. K. Maurice and R. C. Buchanan)
8. Chicago-Milwaukee Section (American Ceramic Society) Jointly With Metals Society (TMS/AIME), Chicago IL., Dec. 12, 1985, "Advances in Modern Technical Ceramics". Invited Lecture.
9. E.I. Dupont de Nemours & Co. Inc., Wilmington DE., Dec. 19, 1985, "Properties Of E-Beam Interactive Oxide Films". Invited Talk.
10. E.I. Dupont de Nemours & Co. Inc., Wilmington DE., Dec. 19, 1985, "Hole Drilling in Thin Ceramic Sheet Substrates By (Nd:YAG) Laser Technique". Invited Talk.

END

FILMED

6-86

DTIC